

# Chapter 8

## Systematics and Prediction in Franck-Condon Factors

Ray Hefferlin, Jonathan Sackett, and Jeremy Tatum

**Abstract** It is the hypothesis of this chapter that diatomic molecular Franck-Condon factors echo the periodicities of atoms. This means that in isoelectronic series, entire Deslandres tables for molecules that are one proton shift away from rare-gas molecules have distinctive behavior relative to other Deslandres tables in the series. An example is in the 21-electron sequence where BeCl, whose chlorine atom is next to the closed-shell magic-number atom argon. The periodicity is found quantitatively and indeed allows for prediction of the vibration frequency for a hypothetical  $^2\Pi$  upper state for CCl.

### 8.1 Introduction

The Franck-Condon factors (FCFs) for the strongest bands of a band system are located in a  $(v',v'')$  table such that a parabola (the Condon locus) often tracks through them [1–3]. The tilt of this parabola, and its latus rectum, can be calculated from the spectroscopic constants of the upper and lower electronic states of the transition. It is relatively rare that the spectroscopic constants and the FCFs are available for any given molecule; the availability is most common for isoelectronic sequences. Hence, we calculate these two properties for the Condon loci of similar band systems for the molecules in isoelectronic sequences. The hypothesis of the work is that these loci will manifest the periodicities of the constituent atoms in the diatomic molecules.

---

R. Hefferlin (✉) • J. Sackett  
Department of Physics, Southern Adventist University, Collegedale, TN 37315, USA  
e-mail: [hefferln@southern.edu](mailto:hefferln@southern.edu)

J. Tatum  
Department of Astronomy, University of Victoria, Victoria, BC V8W 2Y2, Canada

Data for a study by Kuz'menko and Chumak [3] showed that the hypothesis is satisfied for  $q(v',v'') = q(0,0)$  in isoelectronic sequences with 14 and 21 electrons; Hefferlin and Kuznetsova [4] showed that the hypothesis is satisfied for transition moments, another measure of band system intensities. In this chapter, we extend the test of the hypothesis to many more band systems.

## 8.2 Theory

The transition of a diatomic molecule from one electronic state to another takes place almost instantaneously, in a time that is very short compared with the period of molecular vibration. That is to say, the transition takes place with virtually no change in internuclear distance. For that reason, a transition can be indicated in energy level diagrams by means of a vertical line.

A vibrating molecule spends more time in its position of greatest extension (greatest internuclear distance) or greatest compression (least internuclear distance), when the speed of the atoms is least, than it does in its equilibrium position, when the relative speed of the atoms is greatest. This is equally true of a classical model or a wave-mechanical model. (In the latter case, the wavefunctions are greatest at the extrema of the motion.)

Here, we provide formulas that will enable the calculation of the Condon locus in terms of molecular constants for parabolic potential energy functions. Figure 8.1 shows schematically the parabolic energy curves of two simple harmonic oscillators and their discrete vibrational energy levels.

We suppose that the parabolas can be represented by the equations

$$T = T'_e + \frac{k'}{2hc}(r - r'_e)^2, \quad (8.1a)$$

$$T = T''_e + \frac{k''}{2hc}(r - r''_e)^2. \quad (8.1b)$$

Here,  $T'_e$  and  $T''_e$  are the electronic contributions to the term values (energy divided by  $hc$ ), and the second terms are the potential energy terms expressed in wave number units ( $\text{m}^{-1}$ ).  $r$  is the internuclear distance, and  $r_e$  is its equilibrium value.  $k$  is the force constant, related to the molecular constant  $\omega_e$  by

$$k = 4\pi^2 mc^2 \omega_e^2, \quad (8.2)$$

and

$$m = \frac{m_1 m_2}{(m_1 + m_2)}, \quad (8.3)$$

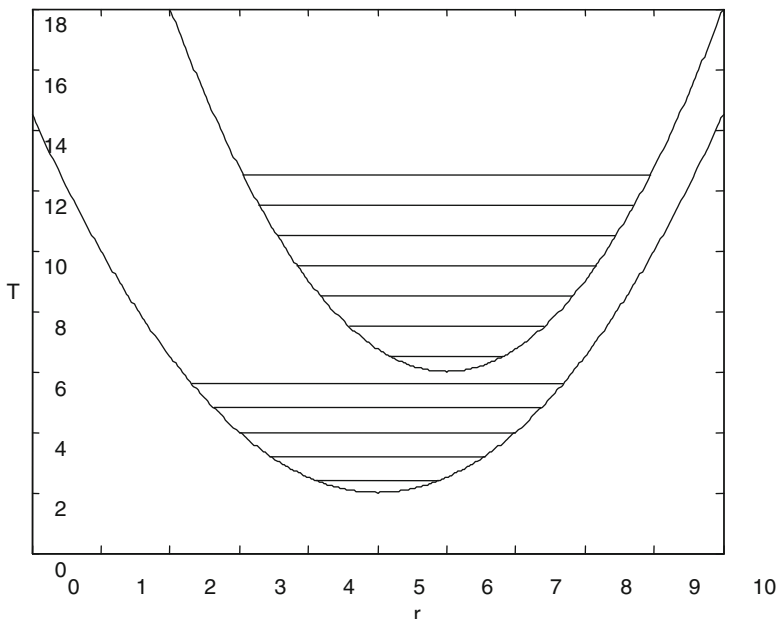


**Fig. 8.1** Potential energy curves of two simple harmonic oscillators and their discrete vibrational energy levels (the numbers on the axes are arbitrary). The vertical separations of the discrete vibrational levels within the two parabolas are inversely proportional to the latera recta of the parabolas. That is to say, the narrower the parabola, the more widely spaced are the vibrational levels

where  $m$  is the “reduced mass” of the molecule. The single primes and the number 1 refer to the upper electronic level, and the double primes and the number 2 to the lower level, in accordance to the usual convention of molecular spectroscopy.

The problem is to draw a horizontal line  $T = T'$  to intersect the upper curve, then to drop vertical lines from the two points of intersection, and finally to find the two values of  $T''$  where these vertical lines intersect the lower curve. It is mathematically straightforward. The line  $T = T'$  intersects the upper curve at  $r$  values given by

$$r = r'_e \pm \sqrt{\frac{2hc}{k'}(T' - T'_e)}. \tag{8.4}$$

The corresponding  $T''$  values in the lower curve are given by

$$T'' = T''_e + \frac{k'}{2hc} \left( r'_e \pm \sqrt{\frac{2hc}{k'}(T' - T'_e)} - r''_e \right)^2. \tag{8.5}$$

We now introduce the term values of the vibrational levels in terms of the vibrational constants  $\omega''_e$  and  $\omega'_e$  via

$$T'' = T_e'' + \left( v'' + \frac{1}{2} \right) \omega_e'' \quad (8.6a)$$

and

$$T' = T_e' + \left( v' + \frac{1}{2} \right) \omega_e' \quad (8.6b)$$

We also make use of

$$k' = 4\pi^2 mc^2 \omega_e''^2 \quad \text{and} \quad k'' = 4\pi^2 mc^2 \omega_e'^2 \quad (8.7)$$

so that

$$\frac{2hc}{k''} = \frac{\hbar}{\pi mc \omega_e''^2} \quad (8.8a)$$

and

$$\frac{2hc}{k'} = \frac{\hbar}{\pi mc \omega_e'^2} \quad (8.8b)$$

The constant  $\hbar/\pi mc$  has the dimension of a length, and we use the symbol  $L$  for it. If  $m$  is expressed in amu,  $L$  has the dimensionless numerical value:

$$L = \frac{6.743052 \times 10^{-17}}{m}. \quad (8.9)$$

Further, we introduce the dimensionless molecular constants

$$\Omega'' = \frac{1}{L\omega_e''}, \quad (8.10a)$$

$$\Omega' = \frac{1}{L\omega_e'}, \quad (8.10b)$$

and

$$\Delta = \frac{r_e'' - r_e'}{L}. \quad (8.11)$$

When these substitutions have been made, we obtain

$$\underline{\underline{\Omega'' \left( v'' + \frac{1}{2} \right) = \left( \Delta \pm \sqrt{\Omega' \left( v' + \frac{1}{2} \right)} \right)^2}}. \quad (8.12)$$

Equation (8.12) is the equation to the Condon parabola in the  $(v'', v')$  plane, in a form that is convenient to compute and to draw. For analysis, it may be more convenient to write it in the standard form for a conic section, namely,

$$\underline{ax^2 + 2hxy + by^2 + 2gx + 2fy + c = 0}, \quad (8.13)$$

in which

$$x = v'' + \frac{1}{2}, \quad (8.14a)$$

$$y = v' + \frac{1}{2}, \quad (8.14b)$$

$$a = \Omega''^2, \quad (8.14c)$$

$$b = \Omega'^2, \quad (8.14d)$$

$$c = \Delta^4, \quad (8.14e)$$

$$f = -\Delta^2 \Omega', \quad (8.14f)$$

$$g = -\Delta^2 \Omega'', \quad (8.14g)$$

$$h = -\Omega'' \Omega'. \quad (8.14h)$$

Equation (8.13) makes it even clearer that Eq. (8.12) describes a parabola. Its axis makes an angle  $\theta$  with the  $v''$  axis;  $\theta$  is given by

$$\text{Tan } \theta = \frac{\omega'_e}{\omega''_e} \quad (8.15)$$

The length  $2l$  of its latus rectum (dimensionless) is

$$2l = \frac{4\Delta^2 \Omega'' \Omega'}{(\Omega''^2 + \Omega'^2)^{3/2}} = \frac{4(r''_e - r'_e)^2 \omega''_e{}^2 \omega'_e{}^2}{L(\omega''_e{}^2 + \omega'_e{}^2)^{3/2}}. \quad (8.16)$$

Several points are of interest. If  $\omega'_e = \omega''_e$ , the angle that the axis of the parabola makes with the  $v''$  axis is  $45^\circ$ , and [3] the parabola degenerates into a straight line. If  $r'_e = r''_e$ , the parabola also becomes a straight line. The vertical and horizontal tangents of the parabola are both at  $v = -0.5$ .

As an example, let us take the following values from [5] for the B-X system of CN:  $m = 6.46427$  amu, so that  $L = 1.04331 \times 10^{-17}$  m

$$r'_e = 1.1506 \times 10^{-10} \text{ m}$$

$$r''_e = 1.1718 \times 10^{-10} \text{ m}$$

$$\omega'_e = 2.16413 \times 10^5 \text{ m}^{-1}$$

$$\omega''_e = 2.068705 \times 10^5 \text{ m}^{-1}$$

In this case,

$$\Delta = 2.0320 \times 10^5$$

$$\Omega' = 4.42898 \times 10^{11}$$

$$\Omega'' = 4.63328 \times 10^{11}$$

The resulting Condon parabola is shown in Fig. 8.2.

### 8.3 Preparation of the Data for Investigations of Isoelectronic Molecules

The obvious starting point would be to compute the data (the angle and the length of the latus rectum) for the Condon locus of the band systems of each fixed-period diatomic molecule (e.g., both atoms from period 2). This procedure suffers from a severe lack of such data. The density of data is greater among isoelectronic series. Table 8.1 shows the isoelectronic series and related data.

For each total electron count, members of isoelectronic sequences were listed in the order  $(Z_1, Z_2)$ , with  $Z_1$  and  $Z_2$  representing the first and second atom in the molecular symbol. In many cases, the atoms are in reverse order compared to standard notation (e.g., SN). The lists were cut into partitions bounded on both ends by a rare-gas molecule. A rare-gas molecule is one having at least one rare-gas molecule (e.g., ONe). A search was made for partitions having at least three members with the same upper and lower state angular momentum quantum number

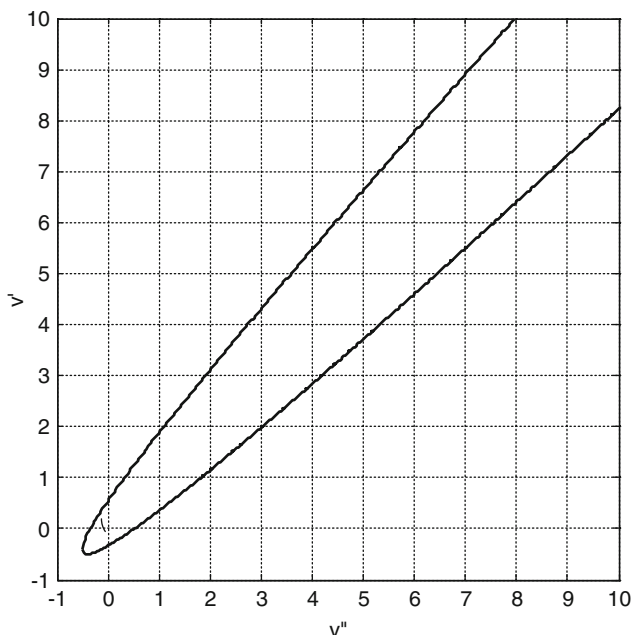


**Fig. 8.2** The Condon locus for the B-X band system of CN with simple harmonic potentials assumed for the *upper* and *lower* states. A Franck-Condon factor lies at each integer intersection. The curve is calculated from the numerical values given in the text. The axis of the parabola makes an angle of  $46.29^\circ$  with the  $v''$  axis, and the length of the latus rectum is  $0.129 v'$  units. In what follows, this Condon parabola would be described as “*narrow*”

and multiplicity and with at least one member no more than one proton shift away from a rare-gas molecule (e.g., BeCl next to BAr). Most of the lower electronic states in the chosen partitions have X designations; the highest encountered upper state is the twelfth above X (including a triplet state), but most have A and B designations. Using FCFs from [5] and spectroscopic constants from [6] for each band system, computation employing the formulas given in Sect. 1.2 provides the latus rectum, the angle  $\theta$ , and a plot of Condon locus. Those with more than three digits after the decimal point have been truncated so that they show three. The scale of the latera recta is the same as that for  $v'$  and  $v''$  in their Deslandres table. CCl is included for purposes of the prediction described in Sect. 8.5. Figure 8.3 shows  $\theta$  for members of an isoelectronic sequence plotted on  $Z_1$ – $Z_2$ .

Some of the symmetry symbols in Table 8.1 are taken from [7] and [8]. The latera recta of the Condon loci in some cases increase along with the  $\theta$  and in the other cases oppositely; in all cases, they behave much more irregularly than do the angles.

**Table 8.1** Total electron count of isoelectronic sequence, member molecules, atomic number difference, spectroscopic constants, latus rectum, and angle of the Condon locus symmetry angle from  $\nu''$

$n_e$	Species	System	$Z_1 - Z_2$	$\omega'_e$ (cm $^{-1}$ )	$r'_e$ (Å)	$\omega''_e$ (cm $^{-1}$ )	$r''_e$ (Å)	Mass (amu)	Latus rectum	Angle
23	AlNe		3							
	SiF	C $^2\Pi-X^2\Pi_r$	5	1031.8	1.529	857.19	1.601	11.315	1.143	50.28
	PO	B $^2\Pi-X^2\Pi_r$	7	759.238	1.717	1,233.34	1.476	10.550	10.516	31.62
	SN	B $^2\Pi_r-X^2\Pi_r$	9 <sup>a</sup>	798.053	1.697	1,218.7	1.494	9.738	7.283	33.22
	CiC	? $\Pi-X^2\Pi$	11 <sup>b</sup>	–	–	866.10	1.645	8.934	–	–
	ArB		13							
23	AlNe		3							
	SiF	B $^2\Sigma^+-A^2\Sigma^+$	5	1,011.23	1.541	718.5	1.605	11.314	0.75	54.6
	PO	A $^2\Sigma^+-B^2\Sigma^+$	7	1,390.14	1.431	1,164.51	1.463	10.548	0.283	39.94
	SN	C $^2\Sigma^+-B^2\Sigma^+$	9	1,389	1.446	1,060	1.49	9.738	0.446	52.65
	CiC		11							
	ArB		13							
22	MgNe		2							
	AlF	A $^1\Pi_r-X^1\Sigma^+$	4	803.94	1.648	802.26	1.654	11.146	0.006	45.06
	SiO	A $^1\Pi_r-X^1\Sigma^+$	6	852.8	1.621	1,241.6	1.510	10.177	2.409	34.48
	PN	A $^1\Pi_r-X^1\Sigma^+$	8	1,103.09	1.547	1,337.2	1.491	9.6434	0.745	39.52
	SC	A $^1\Pi_r-X^1\Sigma^+$	10	1,073.4	1.574	1,285.1	1.535	8.7252	0.319	39.87
	CiB	A $^1\Pi_r-X^1\Sigma^+$	12	849.04	1.689	839.12	1.715	8.3732	0.100	45.34
	ArBe		14							
21	LiAr		15							
	BeCl	A $^2\Pi_r-X^2\Sigma^+$	13	822.11	1.8211	846.7	1.7971	7.166	0.072	44.16
	BS	A $^2\Pi_r-X^2\Sigma^+$	11	752.61	1.8182	1,180.2	1.6092	8.189	6.104	32.53
	CP	A $^2\Pi_r-X^2\Sigma^+$	9	1,061.99	1.653	1,239.7	1.5622	8.649	1.686	40.59
	NSi	A $^2\Pi_r-X^2\Sigma^+$	7	1,044.41	1.6357	1,151.4	1.5719	9.332	0.867	42.21
	OAl	A $^2\Pi_r-X^2\Sigma^+$	5	728.5	1.7708	979.23	1.6179	10.042	3.896	36.65
	FMg	A $^2\Pi_r-X^2\Sigma^+$	3	743.06	1.7469	711.69	1.75	10.610	0.002	42.24





Table 8.1 (continued)

$n_e$	Species	System	$Z_1-Z_2$	$\omega'_e$ (cm $^{-1}$ )	$r'_e$ (Å)	$\omega''_e$ (cm $^{-1}$ )	$r''_e$ (Å)	Mass (amu)	Latus rectum	Angle
BeNe										
14	BeNe									
	BF	$b^3\Sigma^+-X^1\Sigma^+$	-4	1,629.28	1.215	1,402.13	1.263	6.970	0.494	49.29
	CO	$a^3\Sigma^+-X^1\Sigma^+$	-2	1,228.6	1.352	2,169.814	1.128	6.856	9.3530	29.52
	N $_2$	$A^3\Sigma_u-X^1\Sigma_g^+$	0 <sup>c</sup>	1,460.64	1.287	2,358.57	1.100	7.001	8.239	31.73
	CO	$a^3\Sigma^+-X^1\Sigma^+$	2	1,228.6	1.352	2,169.814	1.128	6.856	9.353	29.52
	BF	$b^3\Sigma^+-X^1\Sigma^+$	4	1,629.28	1.215	1,402.13	1.263	6.970	0.494	49.29
BeNe										
13	CN		-1							
	NC	$B^2\Sigma^+-X^2\Sigma^+$	1	2,163.9	1.150	2,068.59	1.172	6.462	0.136	42.29
	OB	$B^2\Sigma^+-X^2\Sigma^+$	3	1,281.69	1.305	1,885.69	1.204	6.521	0.112	34.2
	FBe	$B^2\Sigma^+-X^2\Sigma^+$	5	1,350.8	1.335	1,247.36	1.361	6.113	1.941	47.28
NeLi										
13	CN		-1							
	NC	$A^2\Pi_1-X^2\Sigma^+$	1	1,812.5	1.233	2,068.59	1.172	6.462	1.000	41.22
	OB	$A^2\Pi_1-X^2\Sigma^+$	3	1,260.7	1.353	1,885.69	1.204	6.521	4.148	33.77
	FBe	$A^2\Pi_1-X^2\Sigma^+$	5	1,154.67	1	1,247.36	1.361	6.113	0.162	42.79
NeLi										
13	CN		-1							
	NC	$A^2\Pi_1-X^2\Sigma^+$	1	1,812.5	1.233	2,068.59	1.172	6.462	1.000	41.22
	SB	$A^2\Pi_1-X^2\Sigma^+$	3	753.61	1.8182	1,180.17	1.609	8.189	6.113	32.56
	BrBe	$A^2\Pi_1-X^2\Sigma^+$	5 <sup>d</sup>	698.5 <sup>c</sup>	1.976	715	1.953	8.089	0.063	44.33
KrLi										
			7							

<sup>a</sup>For SN,  $\omega'_e$  is an average of two almost equal numbers (these notes all relate to data in [5])

<sup>b</sup>The ground state of CCl is  $X^2\Pi_{3/2}$  and  $X^2\Pi_{1/2}$ ; the average  $\omega'_e$  is given in the table. No  $\Pi$  or  $\Sigma$  excited state is listed

<sup>c</sup>The lowercase and uppercase designations of the upper states do not agree with Laporte rule

<sup>d</sup>Dubious state assignment

<sup>e</sup>Average of two very close data

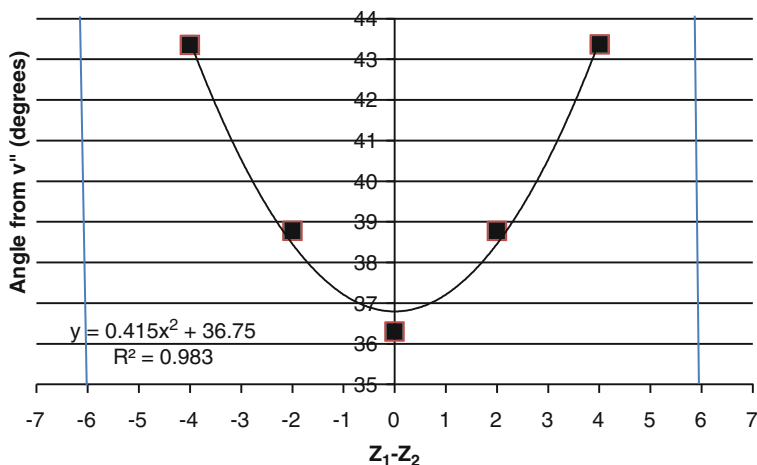


**Fig. 8.3** The angle  $\theta$  of the Condon loci for the 14-electron  ${}^3\Pi^+ - {}^1\Sigma^+$  portion of Table 8.1. For these unusually well-behaved band systems, the Condon loci are very wide in the *center*, *wide*, and *narrow* from center to end. The excited states for  $N_2$  (center), CO, and BF (ends) are the second, fifth, and second states above the ground state

## 8.4 Fitting Errors and Pitfalls in the Data

Plots for 11 isoelectronic sequences having more than three data, or having three centered on  $|Z_1 - Z_2| = \text{zero}$ , were prepared, one of which is shown in Fig. 8.3. Six of the plots have six data points, and three more have five points (one in the center and two duplicated on each side); the remainder have three non-redundant points. The average standard deviation of fitting for these is  $2.595^\circ$ . Figure 8.4 has the largest scatter around its trend line ( $\sigma = 3.951^\circ$ ), so it is used as an example of what the  $(n - 1)$  standard deviations look like. There is no theoretical basis for using quadratic trend lines; they are used for sake of simplicity.

There is no evident correlation between the scatter in the graphs (estimated by eye or calculated as standard deviations), the violation of the rule forbidding multiplicity changes during transitions, the upper electronic states being close to or far above the ground states, the lower electronic states not being ground states, or even the extent to which the two state designations are the same.

## 8.5 A Predicted Upper State Vibration Frequency

It is possible to predict the upper  ${}^2\Pi$ -state vibrational frequency of CCl (top portion of Table 8.1) by finding  $\theta$  from the trend-line equation of the fitting parabola in the figure appropriate to that sequence (not shown). Eq. (8.15) gives  $\omega'_c$  as

$$\omega' = \omega''_c \tan \theta \quad (8.17)$$

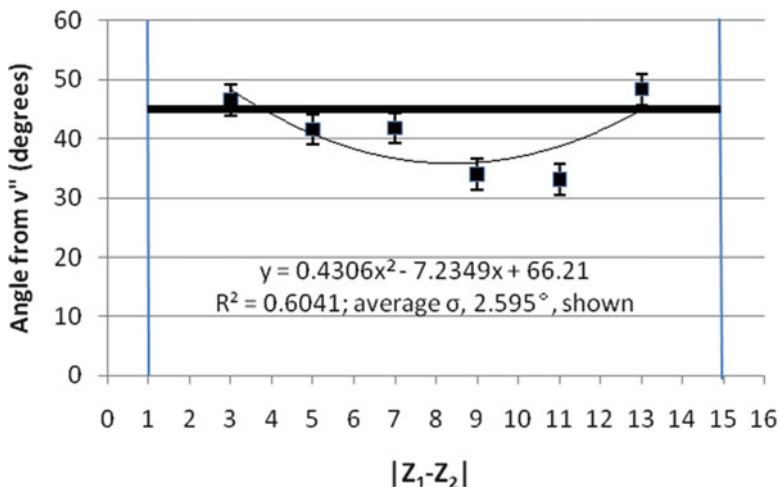


**Fig. 8.4** The angles of the Condon loci for the least well-behaved sequence, the  $\Sigma$ - $\Sigma$  partition of the 21-electron molecules in Table 8.1. The parabola minimum is at  $Z_1 - Z_2 = 8.401$ . The data are provided with average  $(n-1)$  standard deviation derived from all sequences with sufficient numbers of points. From *left to right*, the loci are *narrow, wide, wide, narrow, wide, and narrow* in appearance

Putting  $x = 11$  into the trend-line equation results in a predicted angle  $\theta$  of  $55.08^\circ$  which, when substituted into Eq. (8.17), yields  $\omega'_c = 1,240 \text{ cm}^{-1}$  for the hypothetical  $^2\Pi$  upper state. Using the average of the six deviations found above,  $2.595^\circ$ , the expected standard deviation of this predicted value is  $9.27\%$ .

## 8.6 Summary

All 11 data plots indicate that the hypothesis of this chapter is correct, i.e., that Franck-Condon factor tables echo the periodicities of the atoms comprising diatomic molecules. The 11 graphs show that in isoelectronic series, entire Deslandres tables that are one proton shift away from rare-gas molecules have a distinctive property relative to other tables in the series. The theory has allowed the prediction of the vibration frequency for the first excited  $^2\Pi$ , as yet undiscovered, state of CCl.

## References

1. Nicholls RW (1982) *J Quant Spectrosc Radiat Transf* 28:481–492
2. Standard JM, Clark BK (1999) *J Chem Ed* 76:1363–1366
3. Kuz'menko NE, Chumak LV (1986) *J Quant Spectrosc Radiat Transf* 35:419–429
4. Hefferlin R, Kuznetsova LA (1999) *J Quant Spectrosc Radiat Transf* 62:765–774

5. Huber KP, Herzberg G (1979) Constants of diatomic molecules; constants of diatomic molecules. Van Nostrand Reinhold, New York
6. Kuz'menko NE, Kuznetsova LA, YuYa K (1984) Factory Franka-Kondona Dvukhatomnykh Molekul. Moscow University Press, Moscow
7. Karthikeyan B (2007) Studies on molecular species identified in solar and allied spectra by spectroscopic techniques. Dissertation, Muderai Kamaraj University, India
8. Shanmugavel R (2007) Investigations on the molecular band spectra of astronomical and chemical environment. Dissertation, Muderai Kamaraj University, India